NF-κB Activation, Dependent on Acetylation/Deacetylation, Contributes to HIF-1 Activity and Migration of Bone Metastatic Breast Carcinoma Cells

Paola Bendinelli,[1] Emanuela Matteucci,[1] Paola Maroni,[2] and Maria Alfonsina Desiderio[1]

[1]Dipartimento di Morfologia Umana e Scienze Biomediche "Città Studi," University of Milan and [2]Istituto Ortopedico Galeazzi, Istituto Di Ricovero e Cura a Carattere Scientifico, Milan, Italy

Abstract

Here, we show that NF-κB-HIF-1 interaction contributed to breast cancer metastatic capacity by means of an incomplete epithelial/mesenchymal transition and influencing migration, as shown in 1833 (human) and 4T1 (mouse) metastatic cells after different stimuli. The 1833 and the transforming growth factor-β1–exposed 4T1 cells showed both epithelial (E-cadherins) and mesenchymal (N-cadherins and vimentin) markers, and common mechanisms contributed to the retention of certain epithelial characteristics and the control of migration. The complex NF-κB-HIF-1 reciprocal regulation and the enhanced c-Jun expression played a functional role in exacerbating the invasiveness of 1833 cells after p50/p65 transfection and of 4T1 cells exposed to transforming growth factor-β1. Twist expression seemed to exert a permissive role also regulating epithelial/mesenchymal transition markers. After c-Src wild-type (Srcwt) transfection, c-Src-signal transducer overexpression in 1833 cells increased HIF-1 transactivating activity and invasiveness, and changed E-cadherin/N-cadherin ratio versus mesenchymal phenotype. The transcription factor pattern and the motile phenotype of metastatic 1833 cells were influenced by p65-lysine acetylation and HDAC-dependent epigenetic mechanisms, which positively regulated basal NF-κB and HIF-1 activities. However, HDAC3 acted as a corepressor of NF-κB activity in parental MDA-MB231 cells, thus explaining many differences from the derived 1833 clone, including reduced HIF-1α and c-Jun expression. Invasiveness was differently affected by HDAC knockdown in 1833 and MDA-MB231 cells. We suggest that acetylation/deacetylation are critical in establishing the bone-metastatic gene signature of 1833 cells by regulating the activity of NF-κB and HIF-1, and further clarify the epigenetic control of transcription factor network in the motile phenotype of 1833 cells. (Mol Cancer Res 2009;7(8):1328–41)

Received 11/26/08; revised 4/8/09; accepted 5/1/09; published OnlineFirst 8/11/09.
Grant support: PRIN 2007 (grant no. 12-25201001-14) from Ministero Istruzione, Università e Ricerca, Ricerca Corrente (grant no. 2.30), and Finalizzato (grant no. RF 06-81) from Ministero della Salute, Italy.
The costs of publication of this article were defrayed in part by the payment of page charges. This article must therefore be hereby marked *advertisement* in accordance with 18 U.S.C. Section 1734 solely to indicate this fact.
Requests for reprints: Maria Alfonsina Desiderio, Dipartimento di Morfologia Umana e Scienze Biomediche "Città Studi," Molecular Pathology Laboratory, School of Medicine, University of Milan, via Luigi Mangiagalli, 31-20133 Milan, Italy. Phone: 39-0250315334; Fax: 39-0250315338. E-mail: a.desiderio@unimi.it

doi:10.1158/1541-7786.MCR-08-0548

Introduction

Metastases represent the main cause of death in cancer patients, but how tumors spread and kill the organism is still largely unknown (1, 2). The key molecular events in breast cancer metastasis are poorly understood. Some models can be used to study the phenotypic and epigenetic changes responsible for bone colonization, and recent advances in the molecular profiling of breast cancer MDA-MB231 clones metastasizing to bone have made it possible to establish the presence of genes that closely correlate with the metastatic phenotype (3, 4). However, few studies have considered how the activities of transcription factor networks are regulated, which would clarify the pathogenesis and behavior of metastases, and identify potential molecular targets for therapeutic strategies.

Increasing evidence indicates that NF-κB activity is critical for metastatic colonization and survival, and osteolysis (5-7). The mechanisms regulating NF-κB activity involve subunit acetylation and interaction with IκBα, which plays a unique role in actively removing the p65-NF-κB subunit from the nucleus by means of nucleocytoplasmic shuttling (8-10).

NF-κB regulates epithelial/mesenchymal transition (EMT; refs. 6, 11), but metastasis does not seem to require complete transition to the mesenchymal phenotype (12). Despite their opposite significance in EMT, the E-box–containing genes E- and N-cadherins and vimentin, undergo indirect via Twist, or direct NF-κB regulation (12). E-box overlaps with the HIF-1 responsive element (HRE; ref. 13). The promoters of the genes specifically regulated in bone metastasis, such as endothelin and CXCR4, contain NF-κB and/or HIF-1 consensus sequence(s) [refs. 4, 14, 15].

We hypothesized the possible involvement of complex transcription factor networks in the bone metastasis phenotype and the role of NF-κB and HIF-1 transcription factors, considering also that metastases seem to maintain some aspects of the epithelial phenotype (12). Molecular gene therapy may take a real advantage from the identification of altered synergic interactions and control mechanisms of NF-κB and HIF-1 activities in an attempt to affect gene expression, prevent metastatic growth and improve patient outcome (5, 16, 17).

NF-κB and HIF-1 are involved in cancer progression (5, 18). The interactions of these transcription factors may link inflammation/tumorigenesis, and tumor/microenvironment (19, 20). HGF and vascular endothelial growth factor of stromal and/or tumor origin may activate HIF-1 in carcinoma cells, also in combination with hypoxic stimulus (21, 22). HIF-1 is the master regulator of oxygen homeostasis, but may be activated independently of oxygen concentrations as

a result of genetic alterations and the dysregulation of growth factor signaling (18, 20, 23). Under normoxic conditions, biological stimuli such as growth factors transcriptionally regulate HIF-1α, the inducible subunit of HIF-1 heterodimer. HIF-1α promoter contains numerous consensus sequences for NF-κB and HIF-1, which allow reciprocal control to maintain an autoregulatory loop in the case of stimuli activating NF-κB in normoxia (21, 24). However, the exact mechanism(s) underpinning NF-κB/HIF-1 interactions in metastatic cells, and the signaling pathways downstream of up-regulated NF-κB have not yet been defined. Twist plays an essential role in tumor metastasis and is regulated by NF-κB and HIF-1 activities (12, 25, 26).

The aim of this study was to examine the molecular and biological characteristics of the human bone metastatic 1833 clone derived from parental highly invasive MDA-MB231 breast cancer cells (3), in an attempt to define some aspects of the metastatic phenotype, and the possible retention of some epithelial characteristics leading to an incomplete EMT. To give value to our working hypothesis and to arrive to a broad interpretation, another metastasis cancer model was used. Mouse 4T1 mammary metastatic cells show an epithelioid phenotype and seem to acquire EMT after transforming growth factor (TGF)-β1 treatment (27). We studied the reciprocal regulation of NF-κB and HIF-1, and its impact on migration in human and mouse models, because complex transcription factor interactions might cause disparate responses to identical stimuli, characterizing the molecular differences between prevalently mesenchymal and prevalently epithelial phenotypes (12). In addition to the different patterns of the transcription factors, their regulation at epigenetic level via acetylation/deacetylation might be important to define the metastatic phenotype (28). So, we investigated lysine acetylation of p50 and p65 NF-κB subunits, and the role of histone deacetylases (HDAC) under conditions of NF-κB activation and c-Src expression. The level of c-Src transducer is elevated in the most aggressive breast carcinomas (29), and seems to regulate NF-κB activity, to increase HDAC3 phosphorylation and to affect HDAC3 nuclear translocation, which may also depend on a decrease in interaction with IκBα (30-32). c-Src overexpression, which is sometimes c-*Jun* dependent, may represent a system regulating cell migration (33). HDACs function as corepressors/coactivators of transcription factors by means of as yet unclear mechanisms, although HDAC3 is a corepressor of NF-κB through the deacetylation of p65 (34, 35).

We found that 1833 cells retained some characteristics of differentiated epithelial cells, i.e., E-cadherins and organized structures in collagen type I, while also showing the moderate expression of N-cadherins and vimentin such as mesenchymal cells. The 1833 cells, endowed with the incomplete EMT, had more similarities with TGF-β1–treated 4T1 cells than with MDA-MB231 mesenchymal cells (36). The enhanced migratory capacity of 1833 cells after p50/p65 transfection, and of TGF-β1–treated 4T1 cells, required NF-κB-HIF-1 interaction increasing Twist levels and changing the ratio of EMT markers. By affecting these critical molecular mechanisms, c-Src expression increased, and HDAC knockdown decreased 1833 cell migration. HDAC-dependent epigenetic mechanisms and p65-lysine acetylation regulated, indeed, NF-κB and HIF-1 activities. None of these regulatory mechanisms was observed in MDA-MB231 cells.

Results

NF-κB Posttranslational Regulation Is Different in Bone Metastatic 1833 and Parental MDA-MB231 Cells

We studied NF-κB transactivation, DNA binding activity, subunit composition, and acetylation at lysine in bone metastatic 1833 in respect to parental MDA-MB231 breast carcinoma cells (Fig. 1). The luciferase activity of the gene reporter driven by the NF-κB multimer was similar in both cell lines. Cotransfection with the super-repressor (ssNFκB), a specific and effective NF-κB inhibitor mutated at IκB-conserved serine residues typically targeted for phosphorylation (37), reduced luciferase activity by 90% in MDA-MB231 cells and by 65% in 1833 cells (Fig. 1A). The NF-κB DNA binding and the transactivating activities were reciprocally consistent (Fig. 1B): super-gelshift experiments revealed p50/50 (*a*), p50/65 (*b*), and p65/65 (*c*) dimers in both cell lines (Fig. 1C). ssNFκB transfection largely reduced the DNA binding of the three dimers in the MDA-MB231 cells, whereas p65/65 DNA binding was less affected in the 1833 cells, thus explaining the decrease in transactivating activity after ssNFκB. Octamer-1 DNA binding was unchanged by the treatments (data not shown).

Regardless of IκB degradation, some posttranslational modifications seemed to be involved in regulating NF-κB activity. The partial insensitivity to ssNFκB of NF-κB-DNA binding and transactivation indicated the possible role of phosphorylation. Moreover, the absence of the p52/RelB complex in supergelshift carried out with p52 and RelB antibodies (data not shown) excluded the noncanonical pathway (9, 10).

We next examined the effects of p50 and p65 (p50/p65) cotransfection, an experimental condition that may enhance intracellular subunit levels and their posttranslational changes by increasing NF-κB activity, as occurs after hypoxia and/or treatment with cytokines such as HGF (38). In both cell lines, p50 protein levels increased in the cytosol and nuclei, whereas cytosolic p65 protein levels remained the same as in the corresponding controls (Fig. 1D). However, p65 accumulated (2-fold) in the nuclei of 1833 but not of MDA-MB231 cells. Furthermore, p65-lysine acetylation increased (1.5-fold) in the nuclei of the 1833 cells, but decreased by 40% in the MDA-MB231 nuclei. In the absence of a specific antibody that recognizes acetylated p65, we used the antibody against acetylated lysine, by establishing with immunoprecipitation experiments that the acetylated band at 64 kDa corresponded to p65 (data not shown; ref. 39). The 51-kDa lysine acetylated band coincided with p50, and increased after p50/p65 cotransfection in the 1833 nuclei (Fig. 1D).

Taken together, these findings clearly indicate that endogenous and exogenous p50 and p65 NF-κB subunits were acetylated in the nuclei of the 1833 clone, thus showing that the regulation of NF-κB activity at posttranslational level was different in invasive and bone metastatic cells.

HDAC3 Regulates NF-κB DNA Binding

We studied the involvement of HDAC epigenetic mechanism(s) in the control of NF-κB activity by transfecting the HDAC3 expression vector. HDAC3 or p50/p65 transfection

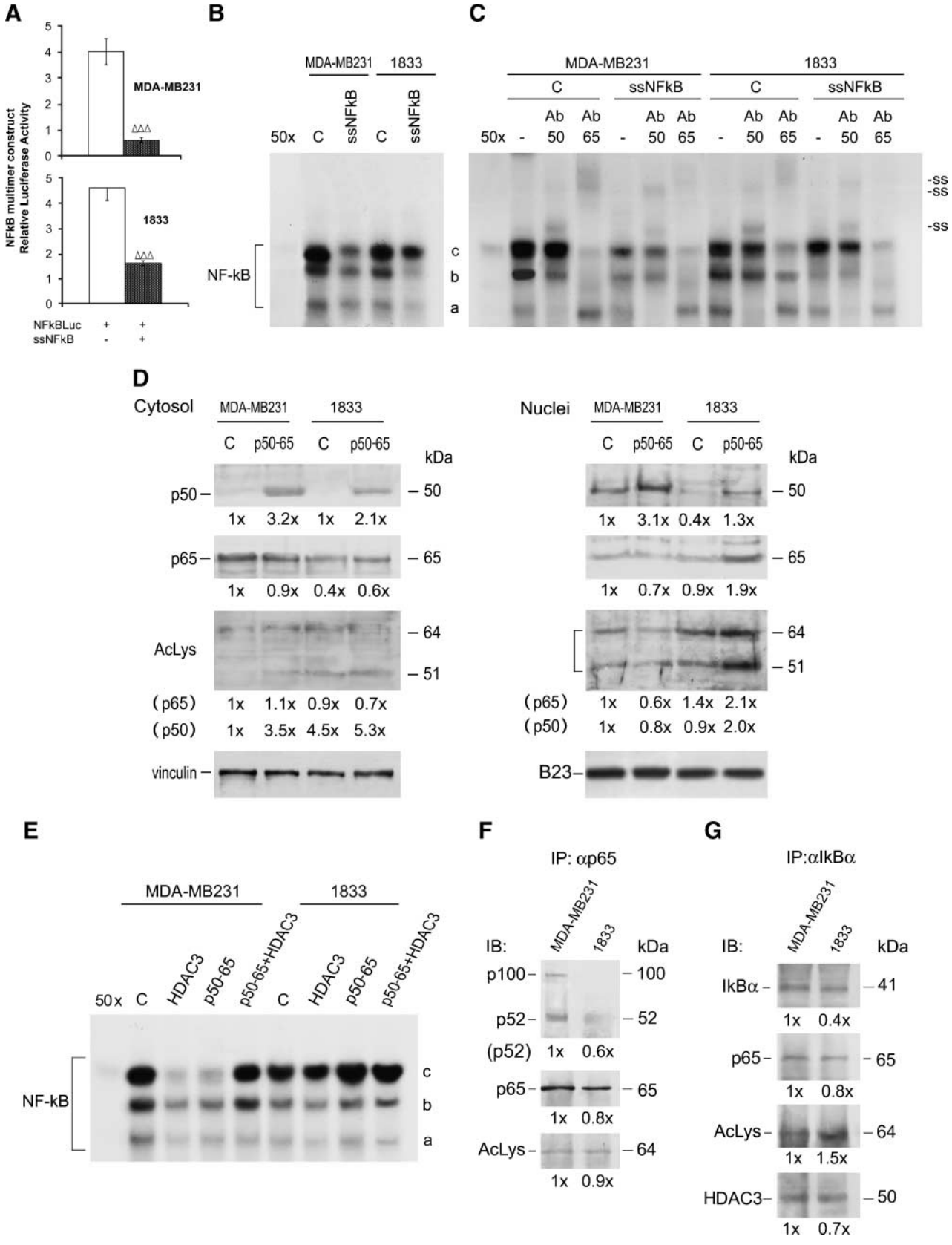

reduced the DNA binding of all of the dimers in the MDA-MB231 cells, and the cotransfection of the three expression vectors caused a reversion that mainly enhanced p50/65 (*b*) and p65/65 (*c*) DNA binding (Fig. 1E). One possible explanation is that HDAC3 overexpression partly reduced the IκBα-Luc promoter activity stimulated by p65, thus decreasing the activity of IκBα, the negative regulator of NF-κB (40). In the 1833 cells, p50/p65 transfection enhanced p65/65 (*c*) DNA binding, whereas HDAC3 had no effect (Fig. 1E). The acetylation status of p65, which decreased in MDA-MB231 and increased in 1833 cells after p50/p65 transfection (see Fig. 1D), might cause the opposite changes in NF-κB DNA binding.

To evaluate the association of the endogenous NF-κB subunits and HDAC3 with IκBα, total cell extracts (500 μg of protein) were immunoprecipitated with anti-p65 or anti-IκBα antibody. In the MDA-MB231 cells, p65 coimmunoprecipitated with p100, and the derived p52 was twice that observed in the 1833 cells (Fig. 1F). Also, p65 as HDAC3 seemed to be less associated with IκBα in MDA-MD231 than in 1833 cells (Fig. 1G).

The association of p65 and IκBα was, therefore, regulated by different mechanisms in the two cell lines: (*a*) competition of p65 with p100 in MDA-MB231 cells (41) and (*b*) p65 acetylation in 1833 cells (40). These mechanisms contributed to the constitutively high level of NF-κB activity, probably because of p65 nuclear retention in both cell lines. It is worth noting that NF-κB transactivating activity was ~20-fold higher in the aggressive breast cancer cells than in the low invasive MCF-7 cells (data not shown).

Role of NF-κB in the Regulation of HIF-1 Activity

To clarify the functional role of NF-κB activity, we studied the expression of HIF-1α and c-*Jun* target genes, and the activity of HIF-1. As shown in Fig. 2A and B, HIF-1α mRNA and protein levels increased (2- to 2.5-fold) in 1833 cells cotransfected with the p50 and p65 expression vectors, c-*Jun* mRNA level tripled, and c-Jun protein level almost doubled in the nuclei but decreased by 70% in the cytosol. Nuclear c-Jun seemed to be phosphorylated as shown by the presence of a slower band. In the cotransfected MDA-MB231 cells, c-Jun mRNA and nuclear-HIF-1α protein levels diminished. The phosphoAkt (pAkt)/Akt ratio increased after p50/p65 transfection only in the 1833 cells (data not shown).

To investigate the effect of c-Jun on c-*Src* promoter activity, 1833 cells were cotransfected with the 0.38SRCLuc and c-Jun or c-Jun-NH_2-terminal kinase (JNK1) expression vectors (Fig. 2C). 0.38SRCLuc activity was reduced by approximately 70% and 50% after c-Jun and JNK1 transfection, respectively. In the same experimental conditions, c-Src protein levels decreased by ~40% (data not shown).

Figure 2D shows that HIF-1 was constitutively active only in the 1833 control cells. Using the labeled HIF-1 oligonucleotide, we observed the specific binding of the dimer containing HIF-1α, and the constitutive binding possibly due to the presence of members of the activating transcription factor/cAMP-responsive element binding protein family (42, 43). The transfection of HDAC3 and p50/p65 respectively reduced and enhanced specific (HIF-1α) DNA binding. Cotransfection of the three gene reporters reduced constitutive binding, possibly because HDAC3 compete for the p300 coactivator (35). The super-gelshift assay using anti–HIF-1α antibody, which gave immunodepletion of the complex, showed the presence of the HIF-1α subunit in the specific DNA binding of HIF-1 (Fig. 2E). Unlabelled activator protein-1 (AP-1) oligonucleotide competed with HIF-1 oligonucleotide binding, but only with regard to the constitutive factor (data not shown). Octamer-1 DNA binding was unchanged by the treatments (data not shown).

To evaluate the role of c-Jun in regulating HIF-1 activity, experiments were done using TAM67 (44), a transactivation-domain deletion mutant of c-Jun that sequesters Jun and Fos family proteins in low activity complexes (45). In 1833 cells, p50/p65 transfection enhanced HRELuc activity 1.6-fold (Fig. 2F). Both basal and induced luciferase activities were largely prevented by TAM67 transfection, thus indicating a possible role of c-Jun in specific and constitutive HIF-1 transactivating activities. These findings are in line with the following: (*a*) possible c-Jun/HIF-1 functional cooperation; (*b*) overlapping of the AP-1 consensus site (first two bases) and the ACGT motif of CRE with HRE (CGTG). In addition to Jun and Fos family members, activating transcription factor/cAMP-responsive element binding protein members bind to AP-1 or other closely related motifs such as CRE (42), and there may be competition for binding to gene promoters (46).

In conclusion, p50/p65 cotransfection induced HIF-1 only in 1833 cells, thus indicating a possible regulatory interaction between NF-κB and HIF-1 activities that may have functional effects on, for example, cell migration.

HIF-1 and c-Jun Were Critical for the Enhanced Migration of 1833 and 4T1 Cells under Various Conditions of NF-κB Induction

On the basis of the above findings, 1833 cells were used to evaluate the functional role of HIF-1 and c-Jun in cell invasiveness after NF-κB induction. The experiments were done using a Matrigel invasion chamber, which is considered to be an *in vitro*

FIGURE 1. Regulation of NF-κB activity in MDA-MB231 and 1833 cells. **A.** The cells were transiently transfected with the gene reporter NFκBLuc in the presence of NF-κB superrepressor (ssNFκB). The histograms indicate the absolute values for Firefly/*Renilla* luciferase activity ratios. Columns, mean of three independent experiments done in triplicate; bars, SEM. $^{\Delta\Delta\Delta}$, $P < 0.001$ versus respective control value. **B.** EMSA analysis of NF-κB using nuclear extracts from control (*C*) and ssNFκB-transfected cells, and (**C**) super-gelshift with specific antibodies (*Ab*) for p50 or p65. ss, supershift; 50×, specific competition with 50-fold excess unlabelled oligonucleotide. The EMSA and super-gelshift experiments were repeated thrice with similar results. **D.** Western blot analysis with cytosol and nuclear extracts from control and p50 plus p65 (p50-65)–transfected cells. Vinculin and B23 were used for normalization of cytosol and nuclear protein levels. The numbers at the bottom indicate the fold-variations relative to MDA-MB231 control value considered as 1. All the experiments were repeated thrice with similar results. **E.** EMSA analysis of NF-κB using nuclear extracts from control and cells transfected with HDAC3 and/or p50-65. 50×, specific competition with 50-fold excess unlabelled oligonucleotide. The experiments were repeated thrice with similar results. **F** and **G.** Immunoprecipitation (*IP*) experiments with total extracts using anti-p65 or anti-IκBα antibody. The numbers at the bottom indicate the fold-variations relative to MDA-MB231 control value considered as 1. The blots shown are representative of three independent experiments.

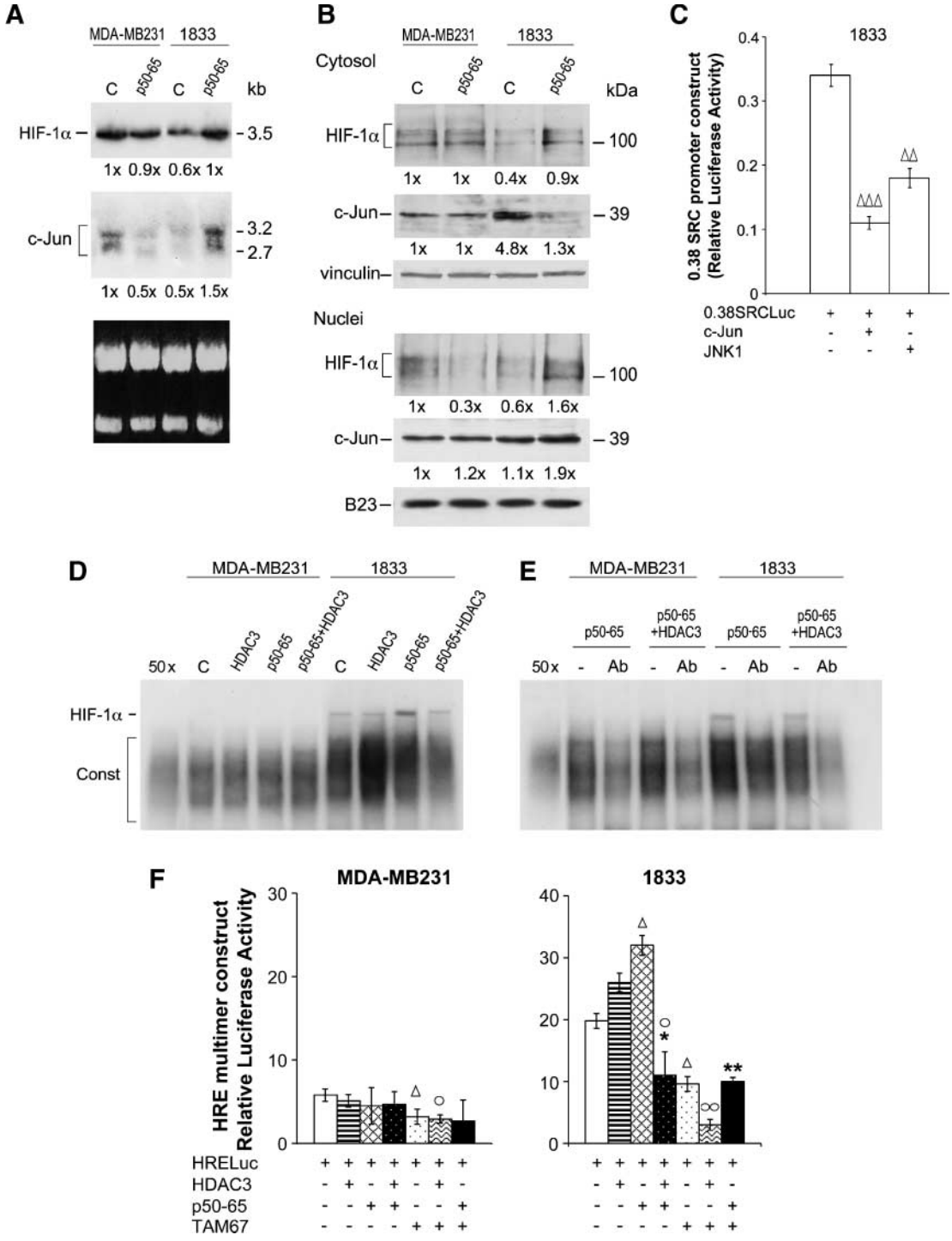

FIGURE 2. Role of NF-κB in the regulation of HIF-1. **A** and **B.** Cells transfected with p50-65 were used to prepare total RNA, cytosolic, and nuclear protein extracts. Equal loading of RNAs was controlled by ethidium bromide staining of rRNAs. Vinculin and B23 were used for normalization of cytosol and nuclear protein levels. The numbers at the bottom indicate the fold-variations relative to MDA-MB231 control value considered as 1. The Northern and Western blots are representative of experiments repeated thrice. **C.** The cells were transiently transfected with 0.38SRCLuc alone or in combination with c-Jun or JNK1 expression vector. The histograms indicate the absolute values for Firefly/*Renilla* luciferase activity ratios. Columns, mean of three independent experiments done in triplicate; bars, SEM. $^{\Delta\Delta}$, $P < 0.005$; $^{\Delta\Delta\Delta}$, $P < 0.001$ versus 0.38SRCLuc-transfected cells. **D.** EMSA analysis of HIF-1 using nuclear extracts from control cells, and from cells transfected with HDAC3 and/or p50-65. HIF-1α, specific binding; const, constitutive binding, and (**E**) super-gelshift with the specific antibody (*Ab*) for HIF-1α. 50×, specific competition with 50-fold excess unlabelled oligonucleotide. The EMSA and super-gelshift experiments were repeated thrice with similar results. **F.** The cells were transiently transfected with HRELuc alone or in combination with the expression vectors indicated. The histograms report the absolute values for Firefly/*Renilla* luciferase activity ratios. Columns, mean of three independent experiments done in triplicate; bars, SEM. $^{\Delta}$, $P < 0.05$ versus corresponding control HRELuc activity value; ○, $P < 0.05$; and ○○, $P < 0.005$ versus HRELuc-HDAC3 cotransfected cells; *, $P < 0.05$; **, $P < 0.005$ versus HRELuc-p50-65 cotransfected cells.

model system for metastasis (38, 47). Representative images of migrated cells are shown in Fig. 3A. The transfection of p50/p65 enhanced cell invasion (~8-fold) through Matrigel in the absence of serum, known to contain growth and chemotactic factors. TAM67 or ΔARNT transfection almost completely prevented the p50/65-dependent increase in the number of migrated cells, but ssNFκB alone or in combination with ΔARNT was less effective, leading to reductions of ~60%. ΔARNT codes for a mutant of the HIF-1β subunit that lacks the basic domain and, although still capable of heterodimerizing with the α subunit, cannot bind DNA (13). TAM67, ssNFκB, or ΔARNT slightly decreased basal cell invasion (data not shown). The ssNFκB data concerning 1833 cell invasion were consistent with the partial inhibition of NF-κB transactivating activity and DNA binding (see Fig. 1).

The studies were extended to another model consisting of metastatic mouse mammary 4T1 cells exposed or not to TGF-β1. As shown in Fig. 3B, the activity of the gene reporter driven by the NF-κB multimer was higher in the 1833 than in the 4T1 cells, whether or not they were cotransfected with p50/p65. In the 4T1 cells treated for 48 hours with TGF-β1, luciferase activity increased 2.8-fold in comparison with the respective control (Fig. 3C).

The 4T1 cells spontaneously migrated through Matrigel, and TGF-β1 increased the migration ~4.5-fold, but concomitant p50/65 transfection did not change the number of migrated cells (Fig. 3D). TAM67 and ΔARNT prevented about 50% and 70% of the TGF-β1–induced migration. It is worth noting that HRELuc activity in the 4T1 cells was similar to that reported for 1833 cells (data not shown).

The data obtained from the two models of metastatic cells, i.e., 1833 transfected with p50/p65 and 4T1 exposed to TGF-β1, confirmed that c-Jun protein and HIF-1 activity downstream of NF-κB were responsible for enhancing motility, although permissive molecular changes might be involved and they were analyzed in the following experiments.

Analysis of EMT Markers in Human and Mouse Breast Carcinoma Models

As shown in Fig. 3E, the EMT markers influencing the motile phenotype of metastatic cells were analyzed in human and mouse breast carcinoma cells. For the mouse model, 4T1 metastatic cells were compared with the completely nonmetastatic tumorigenic 68H cells, with an epithelial phenotype, which did not spontaneously migrate through Matrigel (data not shown). The E-cadherin epithelial marker was markedly expressed in the 68H, less in 4T1 and 1833 cells, and not expressed in the MDA-MB231 cells. The N-cadherin and vimentin mesenchymal markers were expressed in all but not the 68H cells, with the MDA-MB231 cells showing the highest vimentin level.

Figure 3F shows that all of the cell lines expressed Twist protein. The levels were 4-fold higher in the 68H cells than in the 4T1 cells (data not shown). After p50/p65 transfection, Twist protein levels increased 2.5-fold in the 1833 cells, and decreased by 40% in the 4T1 cells. It is worth noting that p50/p65-induced Twist appeared as a diffuse pattern of multiple bands in 1833 cells, possibly due to phosphorylation (48). The opposite changes in Twist protein levels might explain why 4T1 cell migration was unchanged by p50/p65 transfection, unlike that of 1833 cells.

TGF-β1 influenced the expression of EMT markers in 4T1 cells, increasing N-cadherin and vimentin 2.5- to 2.8-fold, and decreasing E-cadherin by 50% (Fig. 3G). It is known that TGF-β1 enhances Twist mRNA expression in 4T1 cells (27), and we also observed an increase in protein level (data not shown).

Involvement of c-Src in Regulating NF-κB and HIF-1 Transactivating Activities

The activity of the gene reporter driven by the multimer of NFκB or HRE was measured after the transfection of c-Src wild-type (Srcwt; Fig. 4), the expression vector for c-Src, which produces the protein and the phosphorylated form depending on cell conditions (31, 49).

Srcwt transfection increased c-Src protein levels ~5-fold in MDA-MB231 and 1833 cells (Fig. 4A), and reduced NFκBLuc activity in both cell lines by about 70% (Fig. 4B). It enhanced basal HRELuc activity (1.7-fold) only in 1833 cells, a stimulatory effect that was prevented by TAM67 (Fig. 4C). These findings confirm the possible role of c-Jun in specific and constitutive HIF-1 transactivating activity in Srcwt-transfected 1833 cells.

To better define c-Src involvement in controlling NF-κB activity, coimmunoprecipitates were obtained using anti-IκBα antibody after Srcwt transfection. As shown in Fig. 4D, Srcwt decreased nuclear IκBα by 40% in the MDA-MB231 cells, and increased it 1.7-fold in 1833 cells: nuclear p65/IκBα association tripled in the MDA-MB231 cells, but did not change in the 1833 cells that, however, showed marked p65-lysine acetylation. IκBα/p65 association also considerably increased in the cytosol of Srcwt-transfected MDA-MB231 cells.

Srcwt enhanced nuclear IκBα/p65 association in MDA-MB231 cells, but caused p65 acetylation in 1833 cells: NF-κB activity therefore diminished, but by means of different mechanisms in the two cell types overexpressing c-Src.

Effect of HDAC 1 and 3 Knockdown on Transcription Factor Activities after Srcwt Transfection

We investigated the involvement of HDACs 1 and 3 in NF-κB and HIF-1 DNA binding under basal conditions and after Srcwt expression by knocking-down the HDACs with the specific siRNAs, which caused the almost complete disappearance of HDAC proteins (Fig. 5A). To check the reproducibility of knockdown, we used two different oligonucleotides for HDAC1: HDAC1.1 and HDAC1.3 (50). HDAC siRNA transfection increased p52 lysine acetylation in the MDA-MB231 cells, which corresponded to the 53-kDa band (Fig. 5B).

In comparison with controls, Srcwt transfection reduced NF-κB DNA binding (except for p65/65; *c*) in the MDA-MB231 cells, whereas the HDAC siRNAs partially reduced all of the bands (Fig. 5C). In the 1833 cells, Srcwt and both HDAC siRNAs largely decreased the NF-κB DNA binding of all of the dimers. These inhibitory effects were partially reversed by Srcwt cotransfection with HDAC siRNAs. The data were confirmed in super-gelshift experiments (Fig. 5D).

As shown in Fig. 5E, Srcwt transfection did not modify practically the specific DNA binding of HIF-1 in 1833 cells.

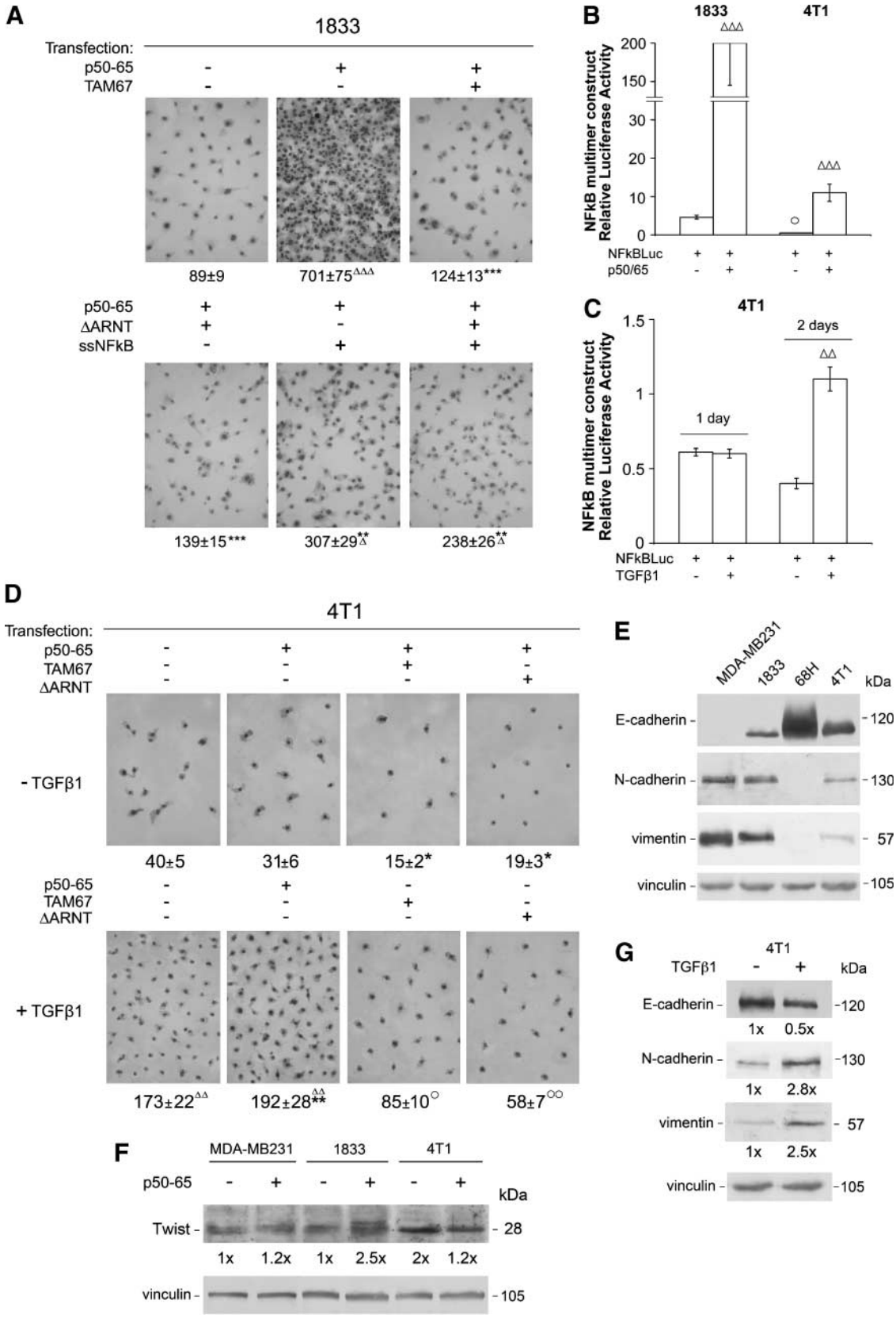

However, the HDAC siRNAs decreased HIF-1 activity (the specific binding of the dimer containing HIF-1α and the constitutive binding) in the controls and after Srcwt transfection of 1833 cells. The presence of the HIF-1α subunit in the DNA binding of the control sample was verified by means of super-gelshift experiments using the specific antibody (Fig. 5E). HDAC1 and HDAC3 knockdown reduced c-Src protein levels by ~50% after Srcwt cotransfection, probably by acting at promoter level (Fig. 5F).

The data relating to NF-κB and HIF-1 transactivating activities in the Srcwt-transfected 1833 cells (Figs. 4 and 5) were largely consistent with those of DNA binding, whereas the data obtained from Srcwt-transfected MDA-MB231 cells suggest that p65/65 was inactive.

Effects of Srcwt and HDACs on the Motile Phenotype

Figure 6A shows the cells grown as three-dimensional cultures in collagen type I gel. MDA-MB231 cells seemed to be separate and spindle shaped (mesenchymal type; ref. 36), rarely forming colonies, whereas the 1833 cells formed more organized colonies similar to tissue structures, probably related to the expression of E-cadherins, and their morphology seemed to be more epithelial than that of the parental cells.

To clarify the influence of the biochemical changes on the biological characteristics of MDA-MB231 and 1833 cells, we did Matrigel invasion assays after Srcwt or HDAC 1 and HDAC 3 siRNA transfection. Srcwt increased the number of migrated 1833 cells by ~3.5-fold, whereas HDAC knockdown was inhibitory (−50%; Fig. 6B). In the Srcwt-transfected 1833 cells, HIF-1α and c-Jun protein levels increased (Fig. 6C); E-cadherin protein level decreased by 50%; and N-cadherin protein level doubled (Fig. 6D). HDAC knockdown in 1833 cells showed opposite effects: it reduced migration (Fig. 6B), increased E-cadherin protein level 4-fold, and decreased N-cadherin protein level by 40% (Fig. 6D). The treatments did not change MDA-MB231 cell invasiveness through Matrigel, in line with the c-Jun reduction by Srcwt and E-cadherin appearance after HDAC knockdown and the generally unchanged levels of the other studied proteins (Fig. 6B, C, and D).

Discussion

The results of this study show the NF-κB-HIF-1 reciprocal regulation that was biologically relevant for migration of human 1833 metastatic clone with bone tropism (3). Tumor cell motility is the hallmark of invasion and an essential step in metastasis, whereas EMT involvement is more controversial and continues to be debated (51).

The following molecular characteristics possibly mediated the 1833 metastatic phenotype, and lacked in parental MDA-MB231 cells: (*a*) the constitutively high level of NF-κB activity, which was up-regulated by the overexpression of the p50 and p65 subunits, with consequent (*b*) HIF-1α induction and HIF-1 activity increase above basal value; (*c*) the p65 lysine acetylation, which increased NF-κB-DNA binding; and (*d*) nuclear c-Jun level enhancement. The up-regulated NF-κB activity in the 1833 cells transactivated HIF-1α and c-Jun, which cooperatively regulated HIF-1 activity and invasiveness. This regulatory interplay was confirmed by experiments using the dominant negative of c-Jun, which largely inhibited HIF-1 transactivating activity. However, the c-Jun/c-Src system did not seem to be relevant to enhance migration of 1833 cells under our experimental conditions. HIF-1α induction implied transcriptional and posttranscriptional mechanisms, possibly favored by the increased pAkt/Akt ratio (Fig. 7; ref. 52).

What may be relevant for the markedly enhanced motile phenotype acquired by 1833 cells after p50/p65 transfection is the possible control of the expression of genes such as matrix metalloproteinase (MMP)1 by HIF-1 (53), probably in cooperation with other important transcription factors for the metastatic phenotype such as Ets1 (54), and the regulation of MMP9 and MMP2 by NF-κB (11).

We examined the validity and the sharing of this complex transcription factor interaction, critical for motile phenotype, and we considered the relationship of the metastatic ability with EMT by using a second experimental model. The fully metastatic 4T1 cells seemed invasive and largely epithelial as they expressed E-cadherins but very little N-cadherins and vimentin; however, exposure to TGF-β1 caused the partial loss of the epithelial phenotype, with reduction of E-cadherin and increase of N-cadherin and vimentin levels. The TGF-β1–induced 4T1 phenotype was therefore quite similar to that of the 1833 metastatic cells, which we can consider an incomplete EMT. The metastatic cells retain, therefore, certain epithelial characteristics (12). In line with this, invasiveness increased in the p50/p65-transfected 1833 cells and in the TGF-β1–treated 4T1 cells. The strong up-regulation of NF-κB activity participated in the enhancement of the motile phenotype, and possibly required the permissive role of Twist and the opposite changes in E-box–regulated proteins of different significance in EMT. The necessity of these concomitant events might explain the different ability of the p50/p65 and TGF-β1 treatments to increase

FIGURE 3. Role of activated NF-κB and downstream signaling pathways in the invasiveness of 1833 and 4T1 cells. **A.** Control (nontransfected) and transfected cells were used for Matrigel invasion assay in the absence of serum in the culture medium added to the chambers. To estimate invasion, we counted (magnification, ×200) the invading cells on the lower side of the membrane after staining. Representative images are shown, and the numbers at the bottom are the mean ± SEM of the counts of 10 selected fields for three independent experiments. $^{\triangle}$, $P < 0.05$; and $^{\triangle\triangle\triangle}$, $P < 0.001$ versus control value; **, $P < 0.005$; and ***, $P < 0.001$ versus p50-65–transfected cells. Cells transiently transfected with NFκBLuc were cotransfected with p50-65 (**B**) or treated with TGF-β1 for 1 or 2 d (**C**). The histograms indicate the absolute values for Firefly/*Renilla* luciferase activity ratios. Columns, mean of three independent experiments done in triplicate; bars, SEM. $^{\triangle\triangle}$, $P < 0.005$; $^{\triangle\triangle\triangle}$, $P < 0.001$ versus respective control value. ○, $P < 0.05$ versus NFκBLuc activity of 1833 control cells. **D.** Control (nontransfected) and transfected cells, exposed or not to TGF-β1 for 2 d, were used for Matrigel invasion assay in the absence of serum in the culture medium added to the chambers. To estimate invasion, we counted (magnification, ×200) the invading cells on the lower side of the membrane after staining. Representative images are shown, and the numbers at the bottom are the mean ± SEM of the counts of 10 selected fields for three independent experiments. $^{\triangle\triangle}$, $P < 0.005$ versus control untreated cells; *, $P < 0.05$; and **, $P < 0.005$ versus p50-65–transfected cells untreated with TGF-β1; ○, $P < 0.05$; and ○○, $P < 0.005$ versus TGF-β1–treated cells. **E, F**, and **G.** Western blot analyses were carried out with total extracts. TGF-β1 treatment was done for 2 d. Vinculin was used for normalization. The numbers at the bottom indicate the fold-variations relative to the control value of MDA-MB231 cells (**F**) or of 4T1 cells (**G**), which were respectively considered as 1. All the experiments were repeated thrice with similar results.

4T1 cell motility. Interestingly, the NF-κB/HIF-1/c-Jun interaction participated in both the spontaneous and TGF-β1–induced 4T1 motile phenotype, as it did in the p50/p65-transfected 1833 cells.

Our data concerning c-Src effects and HDAC epigenetic regulation add mechanistic insights into the role of NF-κB and HIF-1 in tumor progression and metastasis.

Under our experimental conditions, c-Src overexpression in 1833 cells increased migration and elicited the phenotypic changes associated with incomplete EMT. In relation to the signaling pathways triggered downstream of c-Src, HIF-1 activity remained high and HIF-1α/c-Jun/N-cadherins were induced although NF-κB-DNA binding decreased, probably because of the inhibitory p65 acetylation at Lys^{122} and Lys^{123} (40). The HIF-1 target gene Twist might affect E-box–regulated proteins, which is probably why N-cadherin/E-cadherin ratio increased in the Srcwt-transfected 1833 cells exacerbating motility.

HDAC knockdown did exactly the opposite to the system consisting of NF-κB and HIF-1 activities and E-box–regulated proteins, by reducing the invasiveness of 1833 cells. We observed important effects of HDACs as corepressors or coactivators depending on the transcription factor and cell type. This was particularly clear in the 1833 cells, in which endogenous HDAC1 and HDAC3 coactivated basal NF-κB and HIF-1 activities, thus possibly participating in Srcwt-induced migration. c-Src expression may make 1833 cells responsive to microenvironmental stimuli acting through tyrosine kinase receptors (12).

Altogether our findings permit to make a comprehensive conclusion on the biochemical changes with biological relevance, underlying the differences between 1833 and MDA-MB231 cells with partial and complete EMT phenotype. EMT probably promotes early events of metastatization, such as cell migration and invasion of the basement membrane and dissemination into the circulation (51). Unlike MDA-MB231 cells, the 1833 cells formed almost organized structures in three-dimensional collagen gel, and the cohesive forces associated with multicellular aggregates might offer advantages for metastasis survival. The expansion of carcinoma cells into surrounding tissue and, even more, the colonization of secondary growth sites are probably not prevented by the presence of E-cadherins, but what is known as mesenchymal to epithelial transition and E-cadherin re-establishment may occur *in vivo* after cell migration to the site of metastasis. New methylations might be favored in 1833 cells with epigenetic plasticity that, for example, regulate Twist and E-cadherin expression (55). Twist seemed to play a role in the progression of breast cancer, and phosphorylation was probably important in controlling its activity under stimuli that enhanced NF-κB and HIF-1 activities.

The 1833 cells were more plastic than the MDA-MB231 cells also because their NF-κB/HIF-1–regulated gene profile might be influenced by different stimuli and epigenetic mechanisms, thus confirming that metastatic cells have the genome instability necessary to adapt to different environments during metastasis spreading (56). Clinicopathologic studies have shown that increased levels of HIF-1α are associated with tumor progression and a poor prognosis in breast cancer patients (17, 57, 58). We suggest the prevalent importance of

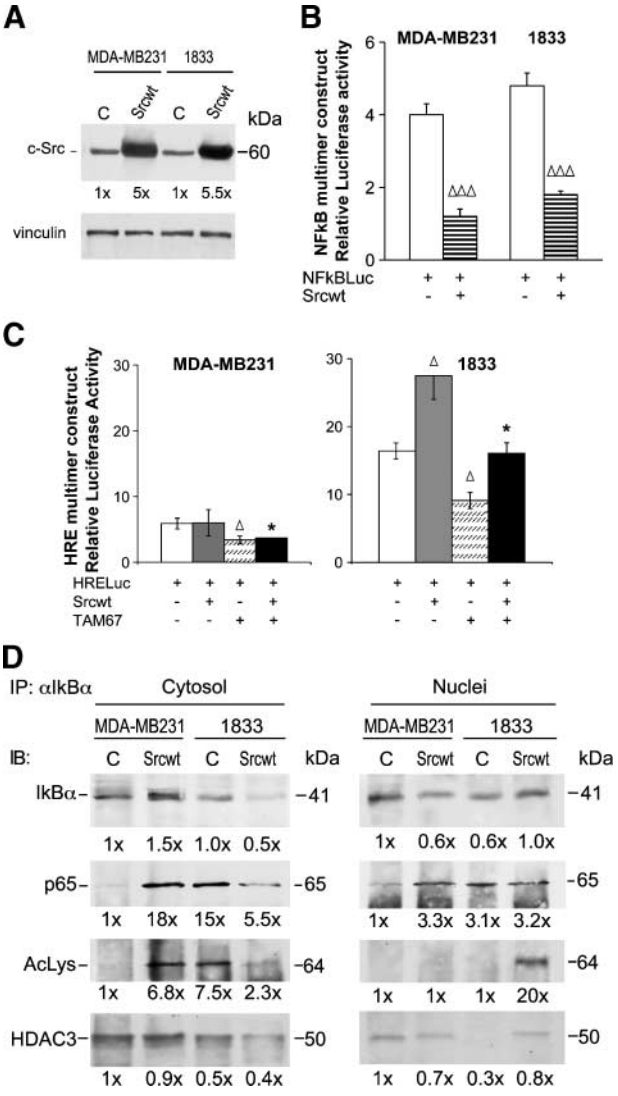

FIGURE 4. c-Src regulates NF-κB and HIF-1 transactivations, and IκBα protein interactions. **A, B,** and **C.** The cells were transiently transfected with the expression vector for Srcwt alone or in combination with NFκBLuc, HRELuc, or TAM67. Western blot analysis was carried out with total extracts, and vinculin was used for normalization. The numbers at the bottom indicate the fold-variations relative to MDA-MB231 control value considered as 1. The Western blot experiments were repeated thrice with similar results. The histograms represent the absolute values for Firefly/*Renilla* luciferase activity ratios. Columns, mean of three (**B**) and six (**C**) independent experiments done in triplicate; bars, SEM. $^{\Delta}$, $P < 0.05$; $^{\Delta\Delta\Delta}$, $P < 0.001$ versus the respective control value; *, $P < 0.05$ versus HRELuc-Srcwt–cotransfected cells. **D.** Immunoprecipitation (*IP*) experiments with cytosolic and nuclear extracts from control or Srcwt-transfected cells using anti-IκBα antibody. The numbers at the bottom indicate the fold-variations relative to MDA-MB231 control value considered as 1. All the experiments were repeated thrice with similar results.

HIF-1 transcription factor activity, which does not always correspond to HIF-1α protein levels. Only the 1833 bone metastatic cells showed an active HIF-1, whereas constitutively expressed HIF-1α cannot form a functional heterodimer with the largely mutated HIF-1β in MDA-MB231 cells (59). Thus, in MDA-MB231 cells the expression of NF-κB/HIF-1 target

genes, which are typical of 1833 bone metastatic cells (3), could be impaired.

Not only HRELuc activity was very low in MDA-MB231 cells, but also p50/65 transfection reduced nuclear NF-κB subunit acetylation at lysine and NF-κB activity. The posttranslational regulation of NF-κB via the lysine acetylation of p65, which primarily occurs in the nuclear compartment, seems to determine the strength and duration of the NF-κB transcriptional response (9) and trigger downstream signaling pathways, which suggests that the persistence of NF-κB activation is critical for HIF-1–dependent transactivation of target genes, not occurring in MDA-MB231 cells.

HDAC knockdown was ineffective on spontaneous invasiveness of MDA-MB231 cells probably because of HDAC3 corepressor function on NF-κB activity. A similar mechanism might be involved in the inhibitory response to Srcwt. As consequence, HIF-1α and c-Jun levels diminished and did not contribute to changes in invasiveness. The p52 lysine acetylation in MDA-MB231 cells knocked down for HDACs, might participate in the reduction of p65/NF-κB DNA binding (39),

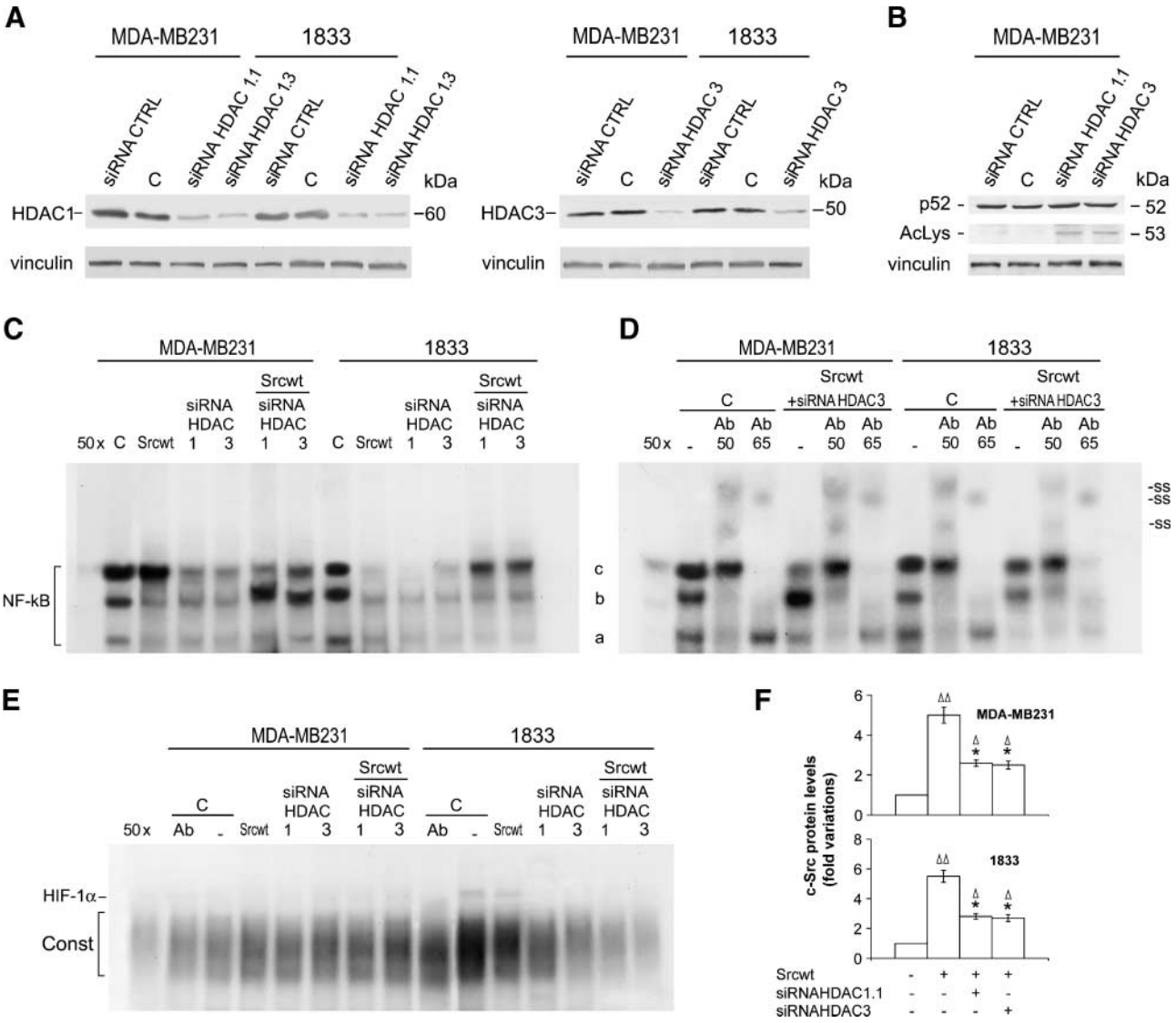

FIGURE 5. Effects of siRNA-mediated knockdown of HDACs 1 and 3 on NF-κB and HIF-1 activities under basal conditions and after Srcwt transfection. **A** and **B.** Western blots of total cell extracts after transfection of siRNA HDAC 1.1, HDAC 1.3, and HDAC 3. As a control (*CTRL*), we used transfection of antiluciferase siRNA. Immunoblots were done with anti-HDAC1, anti-HDAC3, anti-p52, and anti–Acetylated Lysine (*AcLys*) antibodies. Vinculin was used for normalization. The blots shown are representative of three independent experiments. **C, D**, and **E.** EMSA analysis and super-gelshift of NF-κB and of HIF-1 were done with nuclear extracts from control cells and cells transfected with HDAC1.1 or HDAC3 siRNA in the presence or the absence of Srcwt. When indicated, the specific antibody (*Ab*) for p50, p65, or HIF-1α was used. HIF-1α, specific binding; const, constitutive binding. ss, supershift; 50×, specific competition with 50-fold excess unlabelled oligonucleotide. The experiments were repeated thrice with similar results. **F.** The histograms report data relative to Western blot analysis of c-Src protein levels in control (nontransfected) cells and in cells cotransfected with Srcwt expression vector and HDAC siRNAs. Columns, mean of three independent experiments done in triplicate; bars, SEM. $^{\Delta}$, $P < 0.05$; $^{\Delta\Delta}$, $P < 0.005$ versus the respective nontransfected cells; *, $P < 0.05$ versus Srcwt-transfected cells.

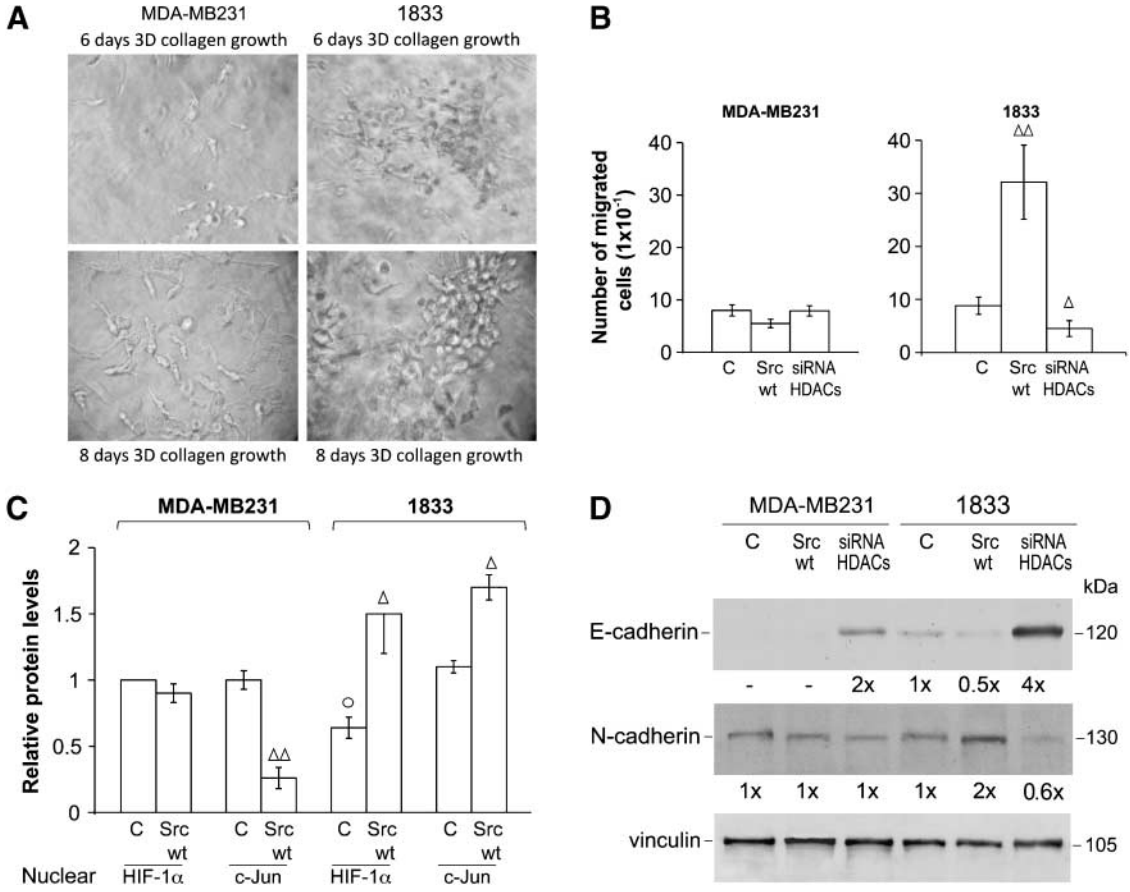

FIGURE 6. Srcwt and HDACs regulated invasiveness of 1833 cells showing incomplete EMT. **A.** Representative images of phase-contrast microscopy of cells, grown in three-dimensional collagen gel for 6 and 8 d, taken at ×200 magnification. The experiments were repeated thrice with similar results. **B.** Control (nontransfected) cells and cells transfected with Srcwt or HDAC (HDAC1.1 plus HDAC3) siRNAs were used for Matrigel invasion assay in the absence of serum in the culture medium added to the chambers. To estimate invasion, we counted (magnification, ×200) the invading cells on the lower side of the membrane after staining. The histograms report the mean ± SEM of the number of migrated cells in 10 selected fields. The experiments have been done in triplicate. $^{\Delta}$, $P < 0.05$; $^{\Delta\Delta}$, $P < 0.005$ versus control value. **C.** Western blots of nuclear extracts from control and Srcwt-transfected cells. The histograms show the fold-variations of protein levels relative to MDA-MB231 control value considered as 1. Immunoblot with vinculin was used for normalization. The experiments were done in triplicate. $^{\Delta}$, $P < 0.05$; and $^{\Delta\Delta}$, $P < 0.005$ versus respective control value; $^{\circ}$, $P < 0.05$ versus MDA-MB231 cell control value. **D.** Western blot analysis was carried out with total extracts from cells transfected with Srcwt or HDAC (HDAC1.1 plus HDAC3) siRNAs, and vinculin was used for normalization. The numbers at the bottom indicate the fold variations relative to 1833 control value considered as 1. All the experiments were repeated thrice with similar results.

suggesting that p52 may be a nonhistone substrate of HDACs (Fig. 8).

Our data underline the fact that the skepticism associated with the targeting of transcription factors needs to be reconsidered: complex regulation of NF-κB and HIF-1 may really influence the molecular signature of bone metastases from human breast cancer, which is different from the invasive phenotype.

Materials and Methods

Materials

Anti–c-Jun (D), anti-NFκB p65 (A), anti-NFκB p50 (NLS), anti-NFκB p52 (C-5), anti-Rel B (C-19), anti–IκB-α (C-21), anti-B23, anti-Twist (H-81), and anti-vinculin antibodies were from Santa Cruz Biotechnology. Anti–HIF-1α antibody for Western blot, anti–E-cadherin (clone 36), anti–N-cadherin (clone 32), and anti-vimentin antibodies, collagen type I, were from BD Pharmingen-Transduction Laboratories. Anti–HIF-1α antibody (OZ15) for super-gelshift was from NeoMarkers-LabVision Corporation. Anti–acetylated-lysine and anti-HDAC3 antibodies were from Cell Signaling. Anti-HDAC1 was from Abcam. Anti-p52 and anti-p100 antibodies were from G. Bonizzi (IEO, Milan, Italy). Recombinant human TGF-β1 was from R&D System. siRNA sequences (a generous gift of S. Chiocca, IFOM, Milan, Italy) were as follows: 5′-CGUACGCGGAAUACUUCGATT-3′ (siRNA LUC, control); 5′-CAGCGACUGUUUGAGAACCTT-3′ (HDAC1.1) and 5′-CUAAUGAGCUUCCAUACAATT-3′ (HDAC1.3) for siRNA HDAC1; and 5′-GAUGCUGAACCAUGCACCUTT-3′ for siRNA HDAC3.

Cell Cultures

The MDA-MB231 human breast carcinoma cells and the derived bone metastatic 1833 clone were a kind gift of J. Massagué (Memorial Sloan-Kettering Cancer Center, New York, NY; ref. 3). Mouse breast carcinoma 68H and 4T1 cells

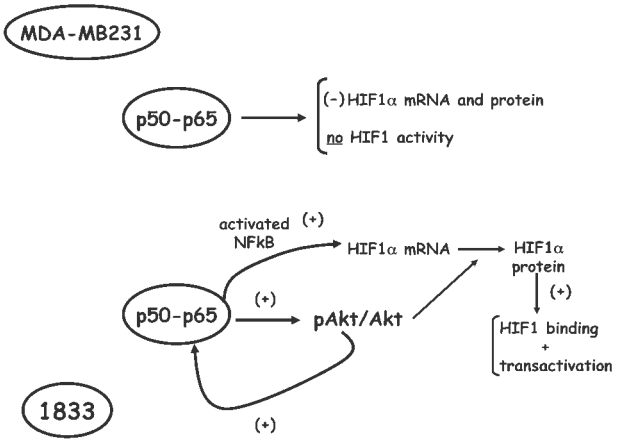

FIGURE 7. Schematic representation of the different control mechanisms exerted by NF-κB (p50-p65) on HIF-1 activity in MDA-MB231 and 1833 cells.

were generously given by F. Miller (Karmanos Cancer Institute, Detroit, MI) and M.P. Colombo (Istituto Nazionale per lo Studio e la Cura dei Tumori, Milan, Italy). Some 4T1 cells were starved overnight and treated with 5 ng/mL TGF-β1 (60).

Plasmids and Cell Transfection

The cells seeded in 24-multiwell plates were transfected (31, 61). The gene reporter plasmid NFκBLuc containing three NF-κB consensus sequences was from M. Hung (Anderson Cancer Center, Houston, TX) and pGL3PGK6TKp containing six HRE was from P.J. Ratcliffe (Welcome Trust Center for Human Genetics, Oxford, United Kingdom); 0.38SRCLuc is the Sca*I*-Hind*III* fragment of the gene reporter construct p0.38SRCA1-CAT (62), subcloned in PGL2-enhancer vector, previously cut with Sma*I* and Hind*III*. For normalization, the cells were transfected with pRL-TK (*Renilla* luciferase) vector, and Firefly/*Renilla* luciferase activity ratios were calculated by the software. The expression vector for HDAC3 was from M. Kovacs (H. Lee Moffitt Cancer Center & Research Institute, Tampa, FL); pCMV-p50 and pCMV-p65 were from W.C. Greene (University of California, San Francisco, CA); Srcwt was from S. Parson (University of Virginia, Charlottesville, VA); pCDNA3-Flag-JNK1 was from R. Davis (Howard Hughes Medical Institute, Worcester, MA); RSVIκBαMSS, coding ssNFκB, was from N.D. Perkins (University of Dundee, Dundee, United Kingdom); pCMVc-Jun and pCMVTAM-67 were from R. Pope (Northwestern University, Chicago, IL); pcDNA3ARNTδ_b (ΔARNT) was from M. Schwarz (Institute for Toxicology, University of Tübingen, Tübingen, Germany). Cells in T75 flasks, transfected with 12.5 μg of Srcwt, were used for the immunoprecipitation experiments; cells in T25 flasks were transfected with 2.5 μg p50, p65, Srcwt, or TAM67, 6.25 μg ΔARNT, and/or 12.5 μg ssNFκB and were used for Northern blots, Western blots, or Matrigel invasion assay.

Transfection of siRNAs

Cells were transfected with 150 nmol/L siRNAs (control, HDAC1, and HDAC3) and/or cotransfected with 2.5 μg Srcwt expression vector using Lipofectamine 2000 in six-multiwell plates. Two cycles of siRNA transfection were done at 24-h interval, and the cells harvested at 72 h were lysed in urea buffer [8 mol/L urea, 0.1 mol/L NaH_2PO_4, 0.01 mol/L Tris (pH 8), and protease inhibitors] to obtain proteins for Western blotting analysis (50), or processed to obtain nuclear extracts for Electrophoretic mobility shift assay (EMSA; ref. 31), or used to perform Matrigel assay.

EMSA Analysis

The sequences of the oligonucleotides for EMSA and supergelshift were as follows: 5′-GGATCCTCAACAGAGGGGACTTTCCGAGGCCA-3′, containing the NF-κB consensus site; 5′-TTCTGATTCGTGCCAAAGCT-3′, containing HRE; and 5′-TGCGAATGCAAATCACTAGAA-3′ containing the Octamer-1 binding site, for loading control (31).

Northern Blot, Immunoprecipitation, and Western Blot Assays

Total RNA (30 μg), or cytosolic (100 μg) and nuclear (50 μg) proteins were used for Northern or Western blots. Total and cytosol extracts (500 μg of protein) or nuclear extracts (100 μg of proteins) were immunoprecipitated with 2 μg of anti-p65 or anti-IκBα antibody (49).

Matrigel Invasion Assay

Invasion assays were carried out essentially as previously described using Matrigel invasion chambers from BD Biocoat Cellware (Becton Dickinson Labware). Transfected cells and TGF-β1–treated cells were harvested, resuspended in medium without serum, added (8×10^4 per well) in triplicate to the upper chambers, and allowed to invade through Matrigel in the absence of serum. The cells that had invaded the lower surface of the membrane were fixed and stained (63).

Collagen Gel Culture

Three-dimensional collage-type I gels were prepared on ice using collagen solution (2.5 mg/mL)/0.5 mol/L HEPES/10×

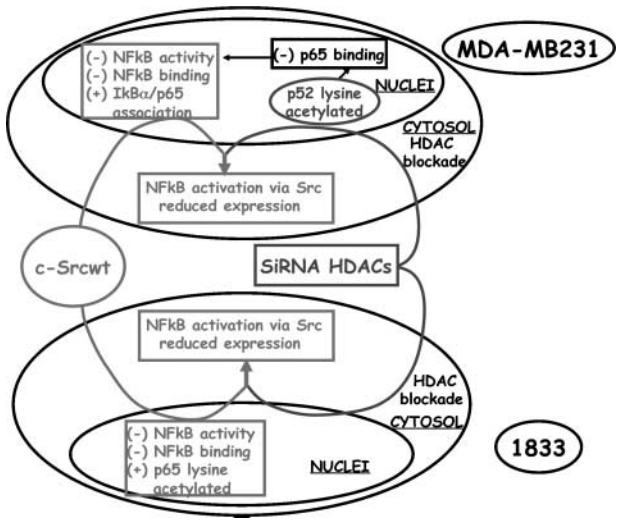

FIGURE 8. Schematic representation of the different mechanisms underlying NF-κB regulation after Srcwt transfection and/or silencing of HDACs in MDA-MB231 and 1833 cells.

DMEM/cell suspension (1×10^5 cells/mL) 7/1/1/1, and allowed to copolymerize at 37°C. Cells (1×10^4) were added to each well of the 96-well plate, and cell culture medium was added above (100 μL containing 20% fetal bovine serum). The plates were incubated at 37°C for 6 to 8 d, at which times complex structures were found. The three-dimensional structures were visualized by phase contrast microscopy (Olympus CKX41).

Statistical Analysis

Luciferase activity and densitometric values were analyzed using ANOVA, with P value of <0.05 considered significant.

Disclosure of Potential Conflicts of Interest

No potential conflicts of interest were disclosed.

Acknowledgments

We thank J. Massagué for 1833 and MDA-MB231 cells (Memorial Sloan-Kettering Cancer Center, New York, NY), S. Pennacchietti (Institute of Cancer Research and Treatment, University of Torino, Italy) for her helpful suggestions concerning the collagen type I experiments, and E. Erba (Istituto di Ricerche Farmacologiche Mario Negri, Milano, Italy) for his microscopy assistance.

References

1. Weigelt B, Peterse JL, van't Veer JL. Breast cancer metastasis: markers and models. Nat Rev Cancer 2005;5:591–602.

2. Gupta GP, Massagué J. Cancer metastasis: building a framework. Cell 2006; 127:679–95.

3. Kang Y, Siegel PM, Shu W, et al. A multigenic program mediating breast cancer metastasis to bone. Cancer Cell 2003;3:537–49.

4. Garcia T, Jackson A, Bachelier R, et al. A convenient clinically relevant model of human breast cancer bone metastasis. Clin Exp Metastasis 2008;25:33–42.

5. Karin M. Nuclear factor-κB in cancer development and progression. Nature 2006;441:431–6.

6. Huber MA, Azoitei N, Baumann B, et al. NF-κB is essential for epithelial-mesenchymal transition and metastasis in a model of breast cancer progression. J Clin Invest 2004;114:569–81.

7. Park BK, Zhang H, Zeng Q, et al. NF-κB in breast cancer cells promotes osteolytic bone metastasis by inducing osteoclastogenesis via GM-CSF. Nat Med 2007;13:62–9.

8. Anguilera C, Fernández-Majada V, Inglés-Esteve J, Rodilla V, Bigas A, Espinosa L. Efficient nuclear export of p65-IκBα complexes requires 14–3-3 proteins. J Cell Sci 2006;119:3695–704.

9. Chen L-F, Greene WC. Shaping the nuclear action of NF-κB. Nat Rev Mol Cell Biol 2004;5:392–401.

10. Perkins ND. Integrating cell-signalling pathways with NF-κB and IKK function. Nat Rev Mol Cell Biol 2007;8:49–62.

11. Min C, Eddy SF, Sherr DH, Sonenshein GE. NF-κB and epithelial to mesenchymal transition of cancer. J Cell Biochem 2008;104:733–44.

12. Christiansen JJ, Rajasekaran AK. Reassessing epithelial to mesenchymal transition as prerequisite for carcinoma invasion and metastasis. Cancer Res 2006;66:8319–26.

13. Dang CV, Semenza GL. Oncogenic alterations of metabolism. Trends Biochem Sci 1999;24:68–72.

14. Maroni P, Bendinelli P, Matteucci E, Desiderio MA. HGF induces CXCR4 and CXCL12-mediated tumor invasion through Ets1 and NF-κB. Carcinogenesis 2007;28:267–79.

15. Farhat N, Matouk CC, Mamarbachi AM, et al. Activation of ET_B receptors regulates the abundance of ET-1 mRNA in vascular endothelial cells. Br J Pharmacol 2008;153:1420–31.

16. Melillo G. Inhibiting hypoxia-inducible factor 1 for cancer therapy. Mol Cancer Res 2006;4:601–5.

17. Milani M, Harris AL. Targeting tumour hypoxia in breast cancer. Eur J Cancer 2008;44:2766–73.

18. Semenza GL. HIF-1 andtumor progression: pathophysiology and therapeutics. Trends Mol Med 2002;8:S62–67.

19. Jung Y-J, Isaacs JS, Lee S, Trepel J, Neckers L. IL-1β-mediated up-regulation of HIF-1α via an NFκB/COX-2 pathway identifies HIF-1 as a critical link between inflammation and oncogenesis. FASEB J 2003;17:2115–7.

20. Desiderio MA. Hepatocyte growth factor in invasive growth of carcinomas. Cell Mol Life Sci 2007;64:1341–54.

21. Tacchini L, De Ponti C, Matteucci E, Follis R, Desiderio MA. Hepatocyte growth factor activated NF-κB regulates HIF-1 activity and ODC expression, implicated in survival, differently in different carcinoma cell lines. Carcinogenesis 2004;25:2089–100.

22. Calvani M, Trisciuoglio D, Bergamaschi CC, Shoemaker RH, Melillo G. Differential involvement of vascular endothelial growth factor in the survival of hypoxic colon cancer cells. Cancer Res 2008;68:285–91.

23. Haddad JJ, Harb HL. Cytokines and the regulation of hypoxia-inducible factor (HIF)1α. Int Immunopharmacol 2005;5:461–83.

24. Görlach A, Bonello S. The cross-talk between NF-κB and HIF-1: further evidence for a significant liaison. Biochem J 2008;412:e17–9.

25. Yang J, Mani SA, Donaher JL, et al. Twist, a master regulator of morphogenesis, plays an essential role in tumor metastasis. Cell 2004;117:927–39.

26. Yang M-H, Wu M-Z, Chiou S-H, et al. Direct regulation of *TWIST* by HIF-1α promotes metastasis. Nat Cell Biol 2008;10:295–305.

27. Lee Y-H, Albig AR, Regner MA, Schiemann BJ, Schiemann WP. Fibulin-5 initiates epithelial-mesenchymal transition (EMT) and enhances EMT induced by TGF-β in mammary epithelial cells via a MMP-dependent mechanism. Carcinogenesis 2008;29:2243–51.

28. Ducasse M, Brown MA. Epigenetic aberrations and cancer. Mol Cancer 2006;5:60–70.

29. Yeatman TJ. A renaissance for Src. Nat Rev Cancer 2004;4:470–80.

30. Huang WC, Chen JJ, Inoue H, Chen CC. Tyrosine phosphorylation of I-κ B kinase α/β by protein kinase C-dependent c-Src activation is involved in TNF-α-induced cyclooxygenase-2 expression. J Immunol 2003;170:4767–75.

31. Matteucci E, Ridolfi E, Maroni P, Bendinelli P, Desiderio MA. c-Src/histone deacetylase 3 interaction is crucial for hepatocyte growth factor-dependent decrease of CXCR4 expression in highly invasive breast tumor cells. Mol Cancer Res 2007;5:833–45.

32. Gao Z, He Q, Peng B, et al. Regulation of nuclear translocation of HDAC3 by IκBα is required for tumor necrosis factor inhibition of peroxisome proliferator-activated receptor γ function. J Biol Chem 2006;281:4540–7.

33. Jiao X, Katiyar S, Liu M, et al. Disruption of c-Jun reduces cellular migration and invasion through inhibition of c-Src and hyperactivation of ROCK II kinase. Mol Cell Biol 2008;19:1378–90.

34. Gao Z, Chiao P, Zhang X, et al. Coactivators and corepressors of NF-κB in IκBα gene promoter. J Biol Chem 2005;280:21091–8.

35. Kasper LH, Brindle PK. Mammalian gene expression program resiliency: the roles of multiple coactivator mechanisms in hypoxia-responsive transcription. Cell Cycle 2006;5:142–6.

36. Wolf K, Mazo I, Leung H, et al. Compensation mechanism in tumor call migration: mesenchymal-amoeboid transition after blocking of pericellular proteolysis. J Cell Biol 2003;160:267–77.

37. Perkins ND. The Rel/NF-κB family: friend and foe. Trends Biochem Sci 2000;25:434–40.

38. Matteucci E, Locati M, Desiderio MA. Hepatocyte growth factor enhances CXCR4 expression favouring breast cancer cell invasiveness. Exp Cell Res 2005; 310:176–85.

39. Hu J, Colburn NH. Histone deacetylase inhibition down-regulates cyclin D1 transcription by inhibiting nuclear factor-*k*B/p65 DNA binding. Mol Cancer Res 2005;3:100–9.

40. Kiernan R, Brès V, Ng RW, et al. Post-activation turn-off of NF-κB-dependent transcription is regulated by acetylation of p65. J Biol Chem 2003;278:2758–66.

41. Dejardin E, Bonizzi G, Bellahcène A, Castronovo V, Merville MP, Bours V. Highly-expressed p100/p52 (NFκB2) sequesters other NF-κ-B-related proteins in the cytoplasm of human breast cancer cells. Oncogene 1995;11:1835–41.

42. Kvietikova I, Wenger RH, Marti HH, Gassmann M. The transcription factors ATF-1 and CREB-1 bind constitutively to hypoxia-inducible factor-1 (HIF-1) DNA recognition site. Nucleic Acid Res 1995;23:4542–50.

43. Agani F, Semenza GL. Mersalyl is a novel inducer of vascular endothelial growth factor gene expression and hypoxia-inducible factor 1 activity. Mol Pharmacol 1998;4:749–54.

44. Alfranca A, Gutiérrez MD, Vara A, Aragonés J, Vidal F, Landázuri MO. c-Jun and hypoxia-inducible factor 1 functionally cooperate in hypoxia-induced gene transcription. Mol Cell Biol 2002;22:12–22.

45. Dong Z, Birrer MJ, Watts RG, Matrisian LM, Colburn NH. Blocking of

tumor promoter-induced AP-1 activity inhibits induced transformation in JB6 mouse epidermal cells. Proc Natl Acad Sci U S A 1994;91:609–13.

46. Manna PR, Stocco DM. Crosstalk of CREB and Fos/Jun on a single *cis*-element: transcriptional repression of the steroidogenic acute regulatory protein gene. J Mol Endocrinol 2007;39:261–77.

47. Liang Z, Yoon Y, Votaw J, Goodman MM, Williams L, Shim H. Silencing of CXCR4 blocks breast cancer metastasis. Cancer Res 2005;65:967–71.

48. Firulli AB, Conway SJ. Phosphoregulation of Twist1 provides a mechanism of cell fate control. Curr Med Chem 2008;15:2641–7.

49. Matteucci E, Ridolfi E, Desiderio MA. Hepatocyte growth factor differently influences Met-E-cadherin phosphorylation and downstream signaling pathway in two models of breast cells. Cell Mol Life Sci 2006;63:2016–26.

50. Senese S, Zaragoza K, Minardi S, et al. Role for histone deacetylase 1 in human tumor cell proliferation. Mol Cell Biol 2007;27:4784–95.

51. Lou Y, Preobrazhenska O, auf dem Keller U, et al. Epithelial-mesenchymal transition (EMT) is not sufficient for spontaneous murine breast cancer metastasis. Dev Dyn 2008;237:2755–68.

52. Sun H-L, Liu Y-N, Huang Y-T, et al. YC-1 inhibits HIF-1 expression in prostate cancer cells: contribution of Akt/NF-κB signaling to HIF-1α accumulation during hypoxia. Oncogene 2007;26:3941–51.

53. Kingsley LA, Fournier PGJ, Chirgwin JM, Guise TA. Molecular biology of bone metastasis. Mol Cancer Ther 2007;6:2609–17.

54. Dittmer J. The biology of the Ets1 proto-oncogene. Mol Cancer 2003;2:1–21.

55. Dumont N, Wilson MB, Crawford YG, Reynolds PA, Sigaroudinia M, Tlsty TD. Sustained induction of epithelial to mesenchymal transition activates DNA methylation of genes silenced in basal-like breast cancers. Proc Natl Acad Sci U S A 2008;105:14867–72.

56. Gao CF, Xie Q, Su YL, et al. Proliferation and invasion: plasticity in tumor cells. Proc Natl Acad Sci U S A 2005;102:10528–33.

57. Hiraga T, Kizaka-Kondoh S, Hirota K, Hiroaka M, Yoneda T. Hypoxia and hypoxia-inducible factor-1 expression enhance osteolytic bone metastases of breast cancer. Cancer Res 2007;67:4157–63.

58. Shim H, Lau SK, Devi S, Yoon Y, Cho HT, Liang Z. Lower expression of CXCR4 in lymph node metastases than in primary breast cancers: potential regulation by ligand-dependent degradation and HIF-1α. Biochem Biophys Res Comm 2006;346:252–8.

59. Wilson CL, Thomsen J, Hoivik DJ, et al. Aryl hydrocarbon (Ah) nonresponsiveness in estrogen receptor-negative MDA-MB231 cells is associated with expression of variant Arnt protein. Arch Biochem Biophys 1997;346:65–73.

60. Neil JR, Schiemann WP. Altered TAB1:IκB kinase interaction promotes transforming growth factor β-mediated nuclear factor-κB activation during breast cancer progression. Cancer Res 2008;68:1462–70.

61. Tacchini L, Matteucci E, De Ponti C, Desiderio MA. Hepatocyte growth factor signaling regulates transactivation of genes belonging to the plasminogen activation system via hypoxia inducible factor-1. Exp Cell Res 2003;290:391–401.

62. Kostyniuk CL, Dehm SM, Batten D, Bonham K. The ubiquitous and tissue specific promoters of the human SRC gene are repressed by inhibitors of histone deacetylases. Oncogene 2002;21:6340–7.

63. Ridolfi E, Matteucci E, Maroni P, Desiderio MA. Inhibitory effect of HGF on invasiveness of aggressive MDA-MB231 breast carcinoma cells, and role of HDACs. Br J Cancer 2008;99:1623–34.